Title : will be set by the publisher
Editors : will be set by the publisher
EAS Publications Series, Vol. ?, 2017

THE FORMATION OF LONG-PERIOD ECCENTRIC BINARIES WITH A HELIUM WHITE DWARF COMPANION

Lionel Siess[1]

Abstract. The recent discovery of long-period eccentric binaries hosting a He-white dwarf has been a challenge for binary-star modelling. Based on accurate determinations of the stellar and orbital parameters for IP Eri, a K0 + He-WD system, we propose an evolutionary path that is able to explain the observational properties of this system and, in particular, to account for its high eccentricity (0.25). Our scenario invokes an enhanced-wind mass loss on the first red giant branch in order to avoid mass transfer by Roche-lobe overflow, where tides systematically circularize the orbit.

1 Introduction

Until recently, binary star calculations were restricted to circular orbits and the problem related to eccentricity was not addressed. However, this is a key ingredient to fully understand the physical mechanisms acting during binary evolution. A tempting parallel can be drawn with single star evolution when we realized that the great achievements of explaining the location of stars in the HR diagram were only revealing the tip of the iceberg and that understanding for their surface composition was much more challenging.

In this contribution, I will illustrate the difficulty to account for the high eccentricity (0.25) of IP Eri, a long period (1071 d) system hosting a helium white dwarf (WD) and a K0 giant.

Stellar evolution tells us that stars with $M \lesssim 0.47 M_\odot$ (e.g. Maeder & Meynet 1989) cannot ignite helium. They are natural progenitors of helium WDs but the problem resides in the lifetime of these objects which exceeds the age of the universe. Therefore, the only valid alternative to explain the formation of a He-WD is to consider a binary scenario. In this paradigm, the initially more massive star looses its H-rich envelope as a result of Roche lobe overflow (RLOF) and leaves

[1] Institut d'Astronomie et d'Astrophysique - Université Libre de Bruxelles (ULB) - CP 226 - 1060 Bruxelles

DOI: (will be inserted later)

an inert helium core of $\sim 0.4 M_\odot$. Depending on the initial period, mass transfer takes place during the main sequence (case A), just after central H depletion (case B) or when the star reaches the red giant branch (late case B). An alternative scenario proposed by Clausen & Wade (2011) involves the merging of the inner stellar components of a hierarchical triple binary to form the He burning star while the outer main sequence companion has no part in this evolution and therefore can have any eccentricity. The problem with this scenario is that the formation of a central He-WD would require the merging of two He WDs whose total mass must not exceed $\sim 0.47 M_\odot$, which is very unlikely. We will therefore focus our investigations on the mass transfer scenario but first, let us describe the physical ingredients needed for this kind of modelling.

2 The modelling of binary stars

To compute the evolution of binary stars, one has to solve the stellar structure equations for each component as well as the evolution of the orbital parameters (separation and eccentricity). Knowledge of the separation yields the size of the Roche radii which determines if the stars are overfilling their Roche lobe and transferring mass. In all the calculations, we use the Eggleton (1983) formulation for the Roche radius (R_{L_1}).

The equation for the evolution of the separation (a) is given by the time derivative of the orbital angular momentum ($J_{\rm orb}$)

$$\frac{\dot{a}}{a} = 2\frac{\dot{J}_{\rm orb}}{J_{\rm orb}} - 2\left(\frac{\dot{M}_d}{M_d} + \frac{\dot{M}_g}{M_g}\right) + \frac{\dot{M}_d + \dot{M}_g}{M_d + M_g} + \frac{2e\dot{e}}{1-e^2} \tag{2.1}$$

where $\dot{M}_{d,g}$ are the mass loss/accretion rates due to RLOF and winds from the donor/gainer and $\dot{e}$ the rate of change of the eccentricity (e). The term $\dot{J}_{\rm orb}$ is given by conservation of the total angular momentum (AM)

$$\dot{J}_\Sigma = \dot{J}_d + \dot{J}_g + \dot{J}_{\rm orb} \tag{2.2}$$

where $\dot{J}_d$ and $\dot{J}_g$ are the torques exerted on each star (due to tides, magnetic braking, mass loss/accretion) and $\dot{J}_\Sigma$ the angular momentum loss rate from the binary which in our case is due to the mass escaping the system. In an evolution where the mass is conserved and the emission of gravitational waves negligible $\dot{J}_\Sigma = 0$. In our modelling, we assume that the matter carries away the same angular momentum per unit mass as resides in the orbital motion of the mass-losing star (this is also referred to as Jean's mode), i.e.

$$\dot{J}_\Sigma = \sum_{i=g,d} \dot{M}_i^{\rm wind} a_i^2 \omega = \left(\frac{\dot{M}_d^{\rm wind}}{q} + q\dot{M}_g^{\rm wind}\right) j_{\rm orb} \tag{2.3}$$

where ω is the orbital angular velocity, a_i the distance of star i to the center of mass of the system ($a_1 + a_2 = a$), $q = M_d/M_g$ the mass ratio and $j_{\rm orb} =$

$J_{\rm orb}/(M_d + M_g)$ the specific orbital AM. In this study, we use the Reimers (1975) prescription for the mass loss rate ($\dot{M}^{\rm wind}$) which is well suited for the evolution of low- and intermediate-mass stars on the RGB. When one of the star overfills its critical equipotential ($R > R_{L_1}$), mass transfer by Roche lobe overflow sets in. To quantify the rate of mass loss from the donor star, we use the Kolb & Ritter (1990) expression which depends on the properties of the stellar surface and orbital separation.

In a binary system, stars are deformed by the gravitational attraction of the companion. The apparition of tidal bulges generate a torque that causes the dissipation of the stars rotational energy and the transfer of angular momentum between the stellar spins and the orbit. As a consequence, the stars first synchronize and on a (much) longer timescale, the orbit circularizes. In his seminal papers, Zahn (1966a,b,c) derived expressions for the torques ($\dot{J}_{d,g}$) and rates of change of the eccentricity ($\dot{e}^{\rm tide}$) in the case of equilibrium and dynamical tides where the energy is dissipated in convective and radiative zones, respectively. This formalism was subsequently refined (Zahn 1977, 1989) and is widely used in binary codes, including the present one.

Tides act to bring the system in a state of minimum energy corresponding to a circular orbit with synchronized spins but if the stars have a mass loss rate that depends on the orbital position, eccentricity is created. As we will see later, this happens when we consider the tidally enhanced wind model and the expression for the eccentricity source term (e.g. Eggleton 2006) is given by

$$\dot{e}^{\rm wind}(\nu) = \frac{|\dot{M}_d^{\rm wind}(\nu) + \dot{M}_g^{\rm wind}(\nu)|}{M_d + M_g} (\cos\nu + e) > 0 \tag{2.4}$$

where ν is the true anomaly and $\dot{M}_i^{\rm wind}$ the (phase dependent) star's wind mass loss rate. It is important to stress that this contribution is always positive and averages to zero if $\dot{M}_i^{\rm wind}$ does not depend on ν. In the end, the equation for the evolution of the eccentricity simply writes

$$\dot{e} = \dot{e}_d^{\rm tide} + \dot{e}_d^{\rm tide} + \dot{e}^{\rm wind} \tag{2.5}$$

Equations (2.1) and (2.5) are solved simultaneously with the stellar structure equations of each component in the BINSTAR code (for details about this modelling, see Siess et al. 2013).

3 The formation of long-period eccentric binaries

3.1 Physical properties of IP Eri

IP Eri is composed of a hot DA WD and a K0IV giant with a period of 1071.00 ± 0.07 days and an eccentricity $e = 0.25$. The analysis of the WD spectra conducted by Burleigh et al. (1997) and Vennes et al. (1998) gives an effective temperature of ~ 30000 K and a gravity $\log g \sim 7.5$. At a distance of $\sim 100\,^{+26}_{-7}$ pc, this leads to an estimated mass of $0.4 \pm 0.03\ M_\odot$ for the hot companion, implying that the white

dwarf is made of He and not of carbon-oxygen. Using high resolution spectra obtained with the HERMES spectrograph mounted on the Mercator telescope at la Palma, Merle et al. (2014) determined the properties of the K0 giant: its composition is nearly solar ([Fe/H] ~ 0.1), the effective temperature $T_{\rm eff} = 4960 \pm 100$ K and $\log g = 3.3 \pm 0.3$. These parameters locate the K0IV giant at the base of the red giant branch (RGB) in the Hertzsprung-Russell diagram and provide a mass estimate ranging between $1.2 - 1.3 \lesssim M_{\rm giant}/M_{\odot} \lesssim 3$. The giant is a slow rotator with $v \sin i < 5$ km s^{-1} and does not show any s-process enhancement confirming that the WD progenitor did not enter the thermally pulsing AGB phase. Indeed, observations of various classes of long-period post-mass transfer systems, including Ba dwarfs, Ba stars or CH stars (for a review, see Jorissen 2003) indicate that a fraction of the AGB wind is accreted by the companion star, resulting in the pollution of its envelope in s-process elements.

Single star calculations done with the STAREVOL code (Siess & Arnould 2008) indicates that the WD entered its cooling track some $\approx 10^7$yr ago. This figure gives us an estimate of the time since the termination of mass transfer and also constrains the initial mass ratio which must have been close to unity so the companion (the K0 giant) can reach the base of the RGB in the short period of time during which the envelope of the WD progenitor is stripped. We also conclude that the WD progenitor must have been initially less massive than $\sim 3M_{\odot}$ because above this limit, stars leave the main sequence with a He core more massive than the WD mass of ~ 0.4M$_{\odot}$.

3.2 The Roche lobe scenario

Standard case A and B mass transfers lead to the formation of systems with a relatively short period like Algols ($P \lesssim 10 - 100$ d). As shown in Fig. 1 for a 1.2+1.0 M$_{\odot}$ system, the initial period must be longer than $\sim$ 300 d to be comparable with that of IP Eri, which implies that mass transfer starts while the star is on the RGB and possesses an extended convective envelope. This late case B RLOF scenario can be problematic if the mass ratio is initially too large. Indeed, the response of a convective star to mass loss is to expand and as long as the mass ratio $q = M_d/M_g > 1$, the separation also shrinks. To avoid a dramatic increase in the mass transfer rate (which grows exponentially with $R - R_{L_1}$) and a subsequent common envelope evolution that would produce a considerable shrinkage of the orbit, the mass ratio must initially be less than $\approx 1.2 - 1.5$ (Webbink 1988). Under these conditions, soon after the start of RLOF, the mass ratio reverts and the orbit begins to widen, stabilizing the mass transfer. In our simulation, the 1.2+1.0 M$_{\odot}$ system detaches after $\sim 5 \times 10^5$ yr when all the giant's envelope has been stripped away, leaving behind a degenerate He core of $\sim 0.37 - 0.43$ M$_{\odot}$. This scenario looks promissing but when we look at the eccentricity, it dramatically fails. In all cases, the orbit circularises and this circularization is always achieved before mass transfer starts. Simplifying the expression for the circularisation timescale derived by Zahn (1978) using a mass ratio close to 1 as required to avoid dynamical RLOF and the formulation of the Roche radius given by Paczyński (1971), it turns out

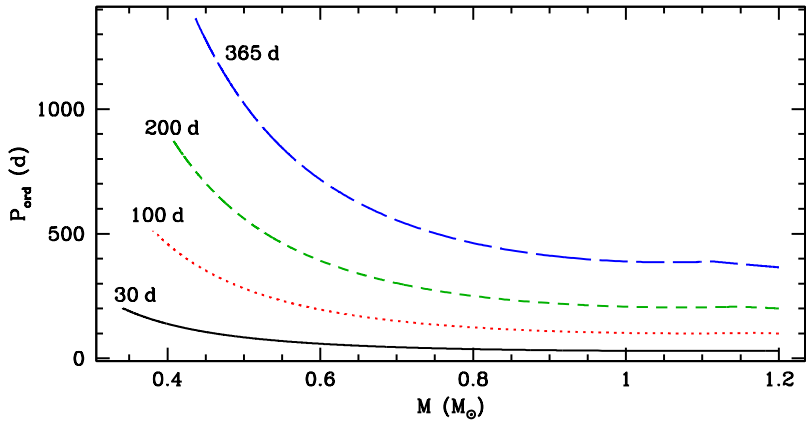

Fig. 1. Evolution (from right to left) of the period for the 1.2+1.0 $M_\odot$ system as a function of the donor's mass during case B mass transfer. The solid, dotted, short- and long-dashed curves correspond to an initial period of 30, 100, 200 and 365 days, respectively.

that

$$\tau_{\rm circ} \approx 4600 \left(\frac{R_{L_1}}{R}\right)^8 \ {\rm yr}\,. \tag{3.1}$$

This timescale is very short in comparison to the evolutionary timescale of a low-mass stars on the RGB. Therefore, as the convective star expands and progressively fills its Roche lobe, dynamical tides will efficiently circularize the orbit before mass transfer begins.

3.3 Tidally enhanced winds

To avoid the circularisation of the orbit during the formation of the He WD, the giant must remain inside its potential well while its enveloppe is removed. One way to achieve this goal is to boost the mass loss rate prior to RLOF. This idea was originally proposed by Tout & Eggleton (1988) to explain the formation of puzzling Algols for which standard evolutionnary channels would imply a dynamically unstable late case B mass transfer. The authors proposed that tides and magnetic acticity are responsible for a substantial increase in the stellar mass loss rate. This way, the Algol system avoids RLOF because the envelope is efficiently lost by the winds. In their simple model, Tout & Eggleton (1988) assume that the wind enhancement factor has the same dependence on the Roche and stellar radii (R/R_{L_1}) as the tidal torque which is supposed to be the driving mechanism. This leads to an effective mass loss rate of the form

$$\dot{M}_i^{\rm wind} = \dot{M}_i^{\rm Reimers} \times \left\{1 + B_{\rm wind} \times \min\left[\left(\frac{R_i}{R_{L_1,i}}\right)^6, \frac{1}{2^6}\right]\right\}\,. \tag{3.2}$$

where $\dot{M}_i^{\rm Reimers}$ is the standard Reimers' mass-loss rate of star i and the constant $B_{\rm wind} \approx 10^4$ was found to match the properties of Z Her, a RS CVn system with a mass ratio below unity. In this expression, the mass loss rate becomes phase dependent because the Roche radius R_{L_1} depends on the instantaneous separation along the eccentric orbit. To follow the secular evolution of the system, over millions of orbits, the equations governing the rate of change of the separation and eccentricity are averaged over an orbital period using a Gaussian quadrature integration scheme. This technique yields mean mass transfer rates (both due to RLOF and winds), mean eccentricity generation terms ($\dot{e}^{\rm wind}$) and torques ($\dot{J}_{\rm orb}$) which are then injected in Eqs. (2.1) and (2.5) (for details, see Siess et al. 2013).

The evolution of the eccentricity as a function of the period for our 1.2+1.0 $M_\odot$ system is presented in Fig. 2. The calculations show that for sufficiently large initial separation, the system can avoid circularisation. Therefore, there is a critical period above which the wind eccentricity pumping term $\dot{e}^{\rm wind}$ dominates over the circularizing tidal contribution $\dot{e}^{\rm tide}$. The analytical determination of this critical initial period where $\int \dot{e}^{\rm wind} dt = -\int \dot{e}^{\rm tide} dt$ is complex because of the phase dependence of the mass loss rate and of the changes of the structure and wind strength of the mass loosing star. Nevertheless, these results indicate that in shorter period systems, tidal interactions tend to dominate over the wind eccentricity generation term.

These primary calculations are encouraging but are still unable to reproduce the eccentricity of IP Eri at a period of 1071 d. This discrepancy may be due to an inadequate choice of the initial conditions which remains to be explored. As

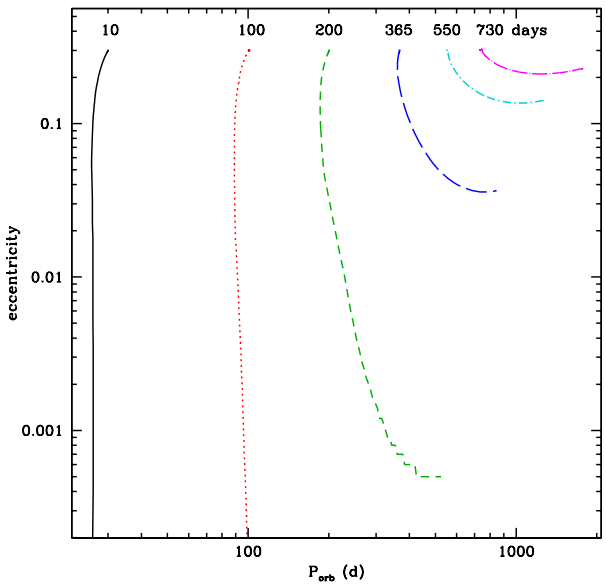

Fig. 2. Evolution of the eccentricity as function of the period for the 1.2+1.0 $M_\odot$ system. The initial eccentricity is set to $e = 0.3$ and the different curves refer to an initial period of 30 (solid), 100 (dotted), 200 (short-dashed), 365 (long-dashed), 550 (dot-short-dashed) and 730 days (dot-long-dashed), respectively.

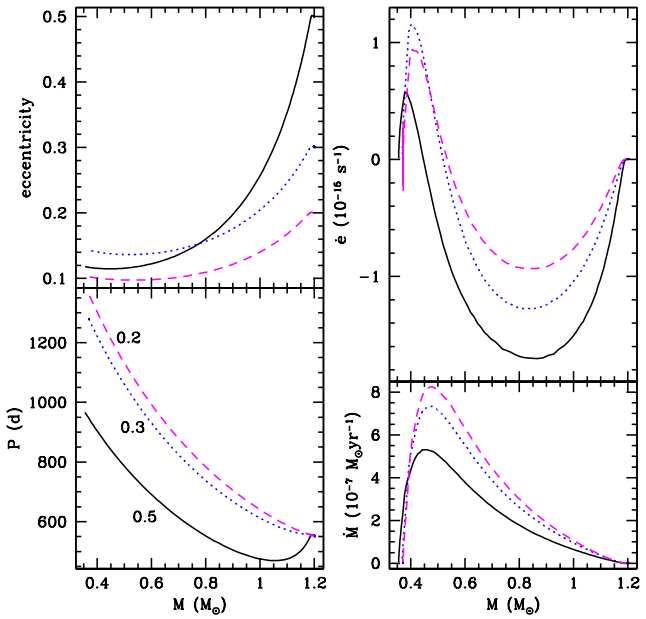

Fig. 3. Evolution as a function of the donor's mass of the eccentricity, period, wind mass loss rate and $\dot{e}$ for the 1.2+1.0 $M_\odot$, 500 d system for 3 different initial eccentricities ($e_{\rm init}$). The solid (black), dotted (blue) and dashed (magenta) lines refer to $e_{\rm init}$ = 0.5, 0.3 and 0.2, respectively.

shown in Fig. 3, increasing our initial eccentricity does not necessarily lead to a more elliptical final orbit. The reason for this behaviour has to do with the phase dependence of the $\dot{e}$ contributions and the fact that quantities are averaged over an orbit. For a given initial period, in systems with a higher eccentricity, the stars get closer to each other at periastron where tides efficiently circularize the orbit but they also spend a larger fraction of their time at greater distances where the eccentricity pumping term dominates. The integration of these effects over an orbit indicate that the average $\dot{M}^{\rm wind}$ (lower right panel in Fig. 3) is smaller when the initial eccentricity is larger, leading to a lower eccentricity pumping efficiency and thus a stronger circularisation. It should also be emphasized that the increase in eccentricity is very modest and only occurs near the end of the evolution when the period has become sufficiently long so tidal interactions are very weak. The increase in the mass loss rate seen in Fig. 3 is due to the giant's expansion in response to mass loss and drops rapidly once the envelope mass has decreased below $\lesssim 0.1 M_\odot$.

The effect of varying the initial masses is illustrated in Fig. 4. For a given companion mass and eccentricity (dotted-red and dashed-green curves in the figure corresponding to $M_g = 1.0 M_\odot$), systems initially more massive end their evolution with a lower eccentricity and a longer period. In both cases, a He-WD of $\sim 0.4 M_\odot$ is formed but a larger amount of material is expelled when the binary hosts a more massive primary. The resulting increase in the period is then a consequence of our adopted Jean's prescription for wind angular momentum loss (Eq.2.3). Indeed,

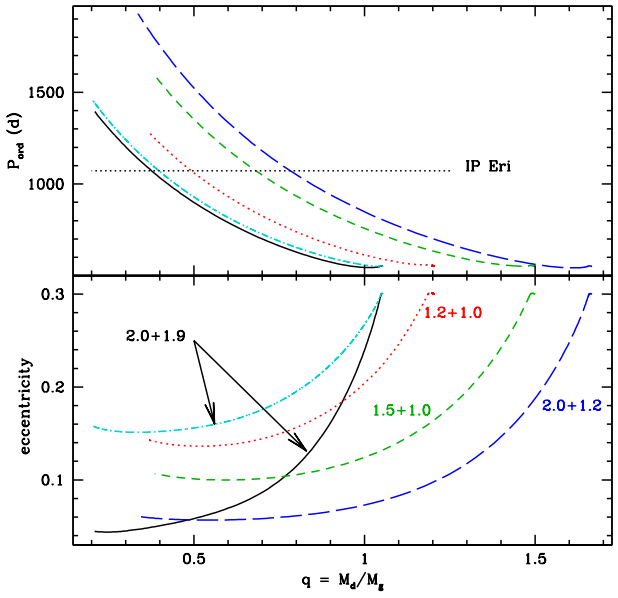

Fig. 4. Evolution of the period and eccentricity as a function of the mass ratio $q = M_d/M_g$ for systems with the same initial period ($P = 550$ d) and eccentricity $e = 0.3$ but with different initial stellar masses. The solid (black), dotted (red), short- (green) and long-dashed (blue) lines refer to the 2.0+1.0 $M_\odot$, 1.2+1.0 $M_\odot$, 1.5+1.0 $M_\odot$ and 2.0+1.2 $M_\odot$ system, respectively. The dotted-dashed (cyan) curve is using $B_{\rm wind} = 2 \times 10^4$ instead of 10^4 by default.

with this formulation, it can easily be shown (e.g. Siess et al. 2014) that the change in the relative system's mass ($d \ln M$) is related to that of the period ($d \ln P$) by

$$d \ln P = -2\, d \ln M \ . \tag{3.3}$$

In our simulations, for the 1.2+1.0 and 1.5+1.0 systems we have respectively $d \ln M = -0.37$ and -0.44 leading to an increase in the period of $d \ln P = 0.73$ and $d \ln P = 0.88$.

Now if we fix the mass of the He-WD progenitor but increase that of the companion (long-dashed-blue and solid-black curves corresponding to $M_d = 2M_\odot$), the system ends up with a shorter final period while keeping a similar eccentricity. In this configuration, the same amount of mass is lost by the giant but in terms of relative mass change ($d \ln M$ in the previous equation) the contribution is smaller for the higher initial mass system. Therefore the period increases is more modest in more massive binaries as shown in the figure. It is worth stressing that the final eccentricity mostly depends on the donor's initial mass because the $\dot{e}$ contributions in Eq. (2.5) mainly come from the donor star ($\dot{e}_d^{\rm tide} \gg \dot{e}_g^{\rm tide}$ and $\dot{e}_d^{\rm wind} \gg \dot{e}_g^{\rm wind}$).

We also played with the parameter $B_{\rm wind}$ which encapsulates our ignorance of the process at the origin of the wind enhancement. This parameter is hard to constrain because it likely depends on the structure of the star and thus varies with time. Considering these large uncertainties (including the *ad hoc* dependence of Eq. 3.2 on R/R_{L_1}), we computed a new model with $B_{\rm wind} = 2 \times 10^4$ instead of 10^4. As expected, increasing $B_{\rm wind}$ boosts the $\dot{e}^{\rm wind}$ term and produces more eccentric systems without significant impact on the final period (Fig. 4)

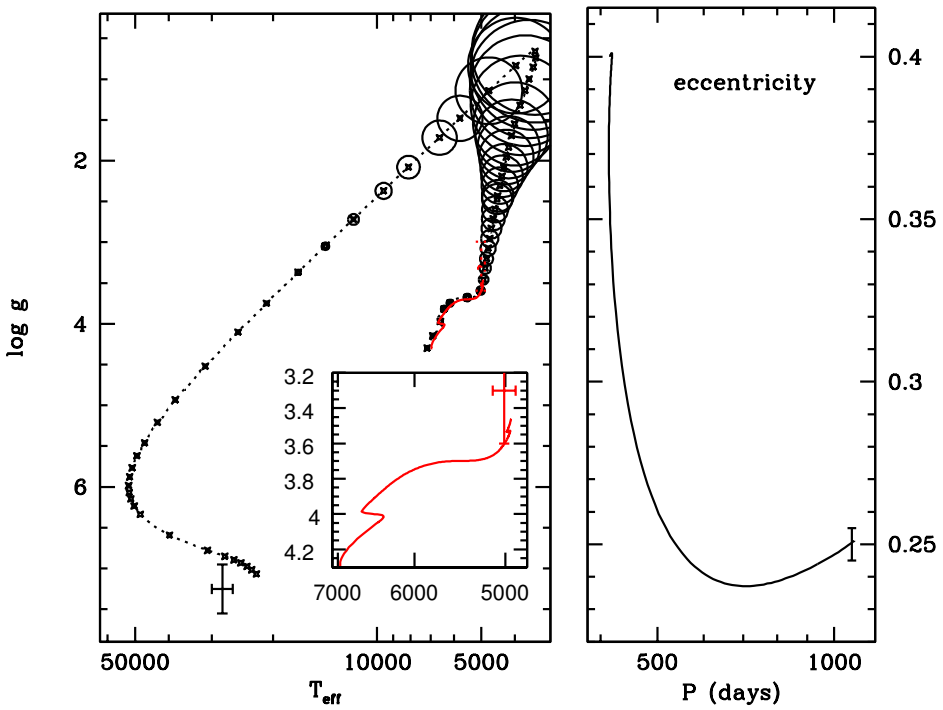

Fig. 5. Evolution of a 1.5 $M_\odot$ (dotted-black curve) + 1.45 $M_\odot$ (solid-red, see also inset) binary with an initial period of 415 d and an eccentricity $e = 0.4$ in the surface gravity - effective temperature (right) and $e - \log P$ (right) diagrams. The locations of the WD and the K0 giant are indicated by the black and red crosses, and the size of the circles is proportional to the progenitor's radius. In this simulation, $B_{\rm wind} = 3.6 \times 10^4$.

The last data to fit is the measured (upper-limit) surface velocity of the giant. In the simulations presented so far, we have not considered the possibility of wind accretion from the He-WD progenitor. For slow winds (≤ 20 km s^{-1}) characteristic of giants, the accretion efficiency is expected to be relatively low, at least in the framework of the Bondi-Hoyle model. This also implies that a small amount of angular momentum is accreted by the gainer star, a fact that is compatible with the slow rotation rate of IP Eri.

The best fit to the observed properties is shown in Fig. 5. It consists of a 1.5+1.45 $M_\odot$ system with an initial period of 415 d, an eccentricity $e = 0.4$ and a wind parameter $B_{\rm wind} = 3.6 \times 10^4$. The location of the stars in the Hertzsprung-Russell and $e - \log P$ diagrams is in very good agreement with the observations. In this simulation, the gainer star has accreted 0.07 $M_\odot$ and the mass of the He-WD is 0.35 $M_\odot$, slightly less than the current estimate. This small discrepancy could be reduced if we had considered core overshooting but one must also realize

that the WD mass estimate is subject to its own uncertainties. Finally, the slow rotation of IP Eri indicates that a small amount of angular momentum has been gained through wind accretion.

4 Conclusion and discussion

Our study of IP Eri showed that stable RLOF during late case B mass transfer leads to the circularisation of the orbit. Furthemore, in this scenario the gainer's rotational velocity is accelerated up to critical values (e.g. Deschamps et al. 2013) that are incompatible with the observations. A successful alternative to maintain a high eccentricity is to consider the tidally enhanced wind model proposed by Tout & Eggleton (1988) and the eccentricity source term given by Eq. (2.4). With these simple prescriptions, we were able to reproduce all the observed features of IP Eri but a physical description of the mechanism behind the wind enhancement is critically lacking.

Recently, Vos et al. (2015) applied this tidally-enhanced wind model to the case of sdB binaries. sdBs are core He-burning stars surrounded by a thin H-rich layer and are also formed as a result of mass transfer during which the envelope of the initially more massive star is ejected. Their internal structure and orbital properties are similar to IP Eri with some long period sdBs exhibiting high eccentricities (e.g. Deca et al. 2012; Barlow et al. 2013). It is therefore tempting to test this scenario on these objects. The simulations of Vos et al. (2015) showed that the tidally enhanced wind model does not work for sdBs because too much mass is removed, resulting in the formation of an inert low-mass helium white dwarfs. The picture is thus more complicated than anticipated but this is not the end of the story. Many other binaries have puzzling eccentricity-period diagrams and the case of barium stars and related Ba dwarfs and CH stars is particularly interesting. These post-mass transfer systems inherited their chemical peculiarity (surface s-process enrichment) from the pollution of a companion that evolved through the AGB and is now an extinct white dwarf. The problem with these systems is similar to the one exposed here : observations (e.g. Van der Swaelmen et al. 2016) show a wealth of eccentric systems in the period range of $500 \lesssim P(d) \lesssim 4000$ where standard tidal theory predicts circular orbits. Several avenues are investigated, including the tidally enhanced wind model and the resonant interaction between a circumbinary disk and the orbit (see the contribution by Jean Teyssandier in this volume) but the problem of maintaining a high eccentricity remains despite the fact that in terms of stellar evolution, we understand reasonably well the structural evolution of both components.

Explaining the eccentricity of binary systems is a new challenge that involves complex processes where tides play a central role. In the late 60's Jean Paul built the foundation of a theory that is still wildly used but the picture is incomplete. We are still lacking a good understanding of the processes and localisation of the dissipation of the tidal energy. We do not know how magnetic fields are impacted by the presence of a companion and despite some attempts (Artymowicz & Lubow 1994), the formation of circumbinary disks and their effects on the orbital param-

eters are still are badly understood. Progress in those directions are needed to explain the evolution of the eccentricity in binary systems.

As a foreword, I would like to say a few word in memory of Jean Paul. My first contact with Jean Paul dates back to 1995. At that time I was a young PhD student and decided to send the draft of my first paper to THE eminent expert for his comments/advise. The text was hardly understandable but Jean Paul very kindly replied with a lot of annotations. Later he honoured my PhD committee by his presence and during my postdoctoral peregrinations, I appreciated his indefensible support and his kindness to write so many letters of recommendations. Later, we collaborated on aspects related to the physics of rotational mixing in low-mass stars. I had the pleasure to meet Jean Paul at several occasions and attend some of his lectures where I could measure and appreciate his pedagogical talents. In addition of being an outstanding scientist and a great teacher, Jean Paul was also a very open minded person gifted with an exceptional human character. I remember a very warm discussion we had one evening at Aussois about the incomparable virtues of Armagnac.

We have lost a great person but his scientific legacy will live on and his spirit will accompany those who had the chance to meet him.

The author acknowledges financial support from the Projet de Recherche PDR T.0198.13 funded by the FRS-FNRS and the organizers of this conference for the invitation. LS is a FNRS senior research associate.

References

Artymowicz, P. & Lubow, S. H. 1994, ApJ, 421, 651

Barlow, B. N., Liss, S. E., Wade, R. A., & Green, E. M. 2013, ApJ, 771, 23

Burleigh, M. R., Barstow, M. A., & Fleming, T. A. 1997, MNRAS, 287, 381

Clausen, D. & Wade, R. A. 2011, ApJ Letters, 733, L42

Deca, J., Marsh, T. R., Østensen, R. H., et al. 2012, MNRAS, 421, 2798

Deschamps, R., Siess, L., Davis, P. J., & Jorissen, A. 2013, A&A, 557, A40

Eggleton, P. 2006, Evolutionary Processes in Binary and Multiple Stars

Eggleton, P. P. 1983, ApJ, 268, 368

Jorissen, A. 2003, in Asymptotic giant branch stars, by Harm J. Habing and Hans Olofsson. Astronomy and astrophysics library, New York, Berlin: Springer, 2003, p. 461, ed. H. J. Habing & H. Olofsson, 461

Kolb, U. & Ritter, H. 1990, A&A, 236, 385

Maeder, A. & Meynet, G. 1989, A&A, 210, 155

Merle, T., Jorissen, A., Masseron, T., et al. 2014, A&A, 567, A30

Paczyński, B. 1971, ARAA, 9, 183

Reimers, D. 1975, Memoires of the Societe Royale des Sciences de Liege, 8, 369

Siess, L. & Arnould, M. 2008, A&A, 489, 395

Siess, L., Davis, P. J., & Jorissen, A. 2014, A&A, 565, A57

Siess, L., Izzard, R. G., Davis, P. J., & Deschamps, R. 2013, A&A, 550, A100

Tout, C. A. & Eggleton, P. P. 1988, MNRAS, 231, 823

Van der Swaelmen, M., Boffin, H. M. J., Jorissen, A., & Van Eck, S. 2016, ArXiv e-prints

Vennes, S., Christian, D. J., & Thorstensen, J. R. 1998, ApJ, 502, 763

Vos, J., Østensen, R. H., Marchant, P., & Van Winckel, H. 2015, A&A, 579, A49

Webbink, R. F. 1988, in Astrophysics and Space Science Library, Vol. 145, IAU Colloq. 103: The Symbiotic Phenomenon, ed. J. Mikolajewska, M. Friedjung, S. J. Kenyon, & R. Viotti, 311

Zahn, J. P. 1966a, Annales d'Astrophysique, 29, 313

Zahn, J. P. 1966b, Annales d'Astrophysique, 29, 489

Zahn, J. P. 1966c, Annales d'Astrophysique, 29, 565

Zahn, J.-P. 1977, A&A, 57, 383

Zahn, J.-P. 1989, A&A, 220, 112

Zahn, J.-R. 1978, A&A, 67, 162